Clays and Clay Minerals, 1969, Vol. 17, pp. 355–371. Pergamon Press. Printed in Great Britain

POLYTYPISM OF TRIOCTAHEDRAL 1:1 LAYER SILICATES

S. W. BAILEY
Department of Geology and Geophysics, University of Wisconsin, Madison, Wisc. 53706

(*Received* 30 *June* 1969)

Abstract—Polytypism in trioctahedral 1:1 phyllosilicates results from two variable features in the structure. (1) The octahedral cations may occupy the same set of three positions throughout or may alternate regularly between two different sets of positions in successive layers. (2) Hydrogen bonding between adjacent oxygen and hydroxyl surfaces of successive layers can be obtained by three different relative positions of layers: (a) direct superposition of layers, (b) shift of the second layer by $a/3$ along any of the three hexagonal X-axes of the initial layer, with a positive or negative sense of shift determined uniquely by the octahedral cation set occupied in the lower layer, and (c) shift of the second layer by $\pm b/3$ along Y_1 (normal to X_1) of the initial layer regardless of octahedral cation sets occupied. Assuming ideal hexagonal geometry, no cation ordering, and no intermixing in the same crystal of the three possible types of layer superpositions, then twelve standard polytypes (plus four enantiomorphs) with periodicities between one and six layers may be derived. Relative shifts along the three X-axes lead to the same layer sequences derived for the micas, namely $1M$, $2M_1$, $3T$, $2M_2$, $2Or$, and $6H$. Polytypes $1T$ and $2H_1$ result from direct superposition of layers. Layer shifts of $b/3$ lead to polytypes designated $2T$, $3R$, $2H_2$, and $6R$. The twelve standard 1:1 structures can be divided into four groups ($A = 1M, 2M_1, 3T$; $B = 2M_2, 2Or, 6H$; $C = 1T, 2T, 3R$; $D = 2H_1, 2H_2, 6R$) for identification purposes. The strong X-ray reflections serve to identify each group and the weaker reflections differentiate the three structures within each group. Examples of all four groups and of 9 of the 12 individual structures have been identified in natural specimens. Consideration of the relative amounts of attraction and repulsion between the ions in the structures leads to the predicted stability sequence group C > group D > group A > group B, in moderately good agreement with observed abundances of these structural groups.

INTRODUCTION

THEORETICAL stacking sequences for trioctahedral 1:1 layer silicates have been derived previously by Steadman (1964), Zvyagin, Mischenko, and Shitov (1966), and Zvyagin (1967) and for dioctahedral species by Newnham (1961) and Zvyagin (1962). The writer has been using a polytype system slightly different than any of the above in his classes since 1957. The results are now presented formally because the notation system is believed to be more convenient for practical usage and because a more detailed presentation had been promised in earlier references to specific polytypes (Bailey, 1963, 1966, 1967).

As in the derivation of the polytypes of the micas (Smith and Yoder, 1956) and of the chlorites (Bailey and Brown, 1962), certain simplifying assumptions are made at the outset. It is assumed that:

(1) successive layers are identical in composition and structure,
(2) the octahedral sheets are trioctahedral so that all three octahedral sites in the smallest structural unit (one hexagonal ring) are occupied,
(3) no cation ordering takes place,
(4) the tetrahedral and octahedral sheets have ideal hexagonal geometry, without distortion,
(5) the stacking of layers is regular rather than random,
(6) the different ways in which individual layers can be stacked, e.g. relative displacements along X, along Y, or no displacement, are not intermixed in the same crystal, and
(7) for the case of relative interlayer displacements along X, the same interlayer stacking angle, e.g. $\pm 60°$ or $\pm 120°$, is found between all the layers.

In practice most natural crystals do not obey all of the foregoing assumptions. This may lead to more complex structures than those derived here and, in some cases to structures that are not truly polytypic, or even polymorphic, with one another. Some of the consequences of deviations from these assumptions will be discussed in later sections of the paper.

SYSTEMATIC DERIVATION OF 12 STANDARD POLYTYPES

General

Within each 1:1 layer octahedral cations can occupy either set I or set II positions above the

tetrahedral sheet, as defined in Fig. 1*a* relative to fixed hexagonal axes. The uppermost plane of hydroxyls then must fit above the occupied I or II sites to form octahedra that slant in opposite directions for the two cases (Fig. 1*b*). It is evident that set I transforms to set II by rotation of the layer by $\pm 60°$ or 180°. The important part in what follows is not which set is occupied, but whether the same set of three octahedral positions is occupied in each successive layer or whether there is an alternation between the I and II sets in successive layers. The latter is equivalent to relative layer rotations.

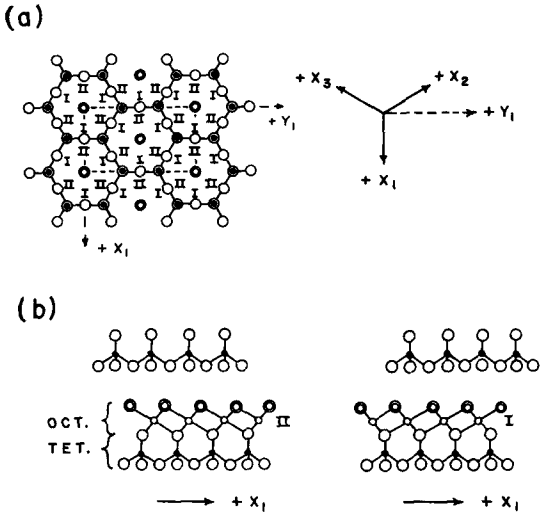

Fig. 1. (a) Definition of I and II sets of octahedral cation positions above the tetrahedral net relative to fixed hexagonal axes. (b) Octahedral sheets slant in opposite directions relative to a fixed X_1 axis due to occupancy of I or II octahedral cation sets.

Polytypism in 1 : 1 layer silicates is more complex than in the micas, because there is no interlayer cation to anchor the relation of successive layers. Adjacent layer positions are now governed by the need for a pairing of each oxygen on the basal tetrahedral surface of one layer with an OH group on the upper octahedral surface of the layer below (Fig. 2). This OH—O pairing results in the formation of long hydrogen bonds, approximately 3·0 Å between the anion centers, that bond the layers together (Gruner, 1932; Hendricks, 1939*a*).

Interlayer hydrogen bonds can be formed from the following three relative positions of adjacent 1 : 1 layers.

(1) No shift of the succeeding layer. The hexagonal rings in the tetrahedral sheets of adjacent layers are exactly superimposed (aside from possible rotations of $\pm 60°$ or 180°).

(2) Shift of the second layer by $a/3$ along the fixed axes X_1, X_2, or X_3 of the initial layer, with or without rotation of the second layer. Because of the different slant of the I and II octahedra the interlayer shift must be in the negative direction if the II octahedral set is occupied in the initial layer, as shown in Fig. 2, or in the positive direction if the I octahedral set is occupied.

(3) Shift of the second layer by $\pm b/3$ along any of the three hexagonal Y axes of the initial layer (normal to the three X axes), with or without rota-

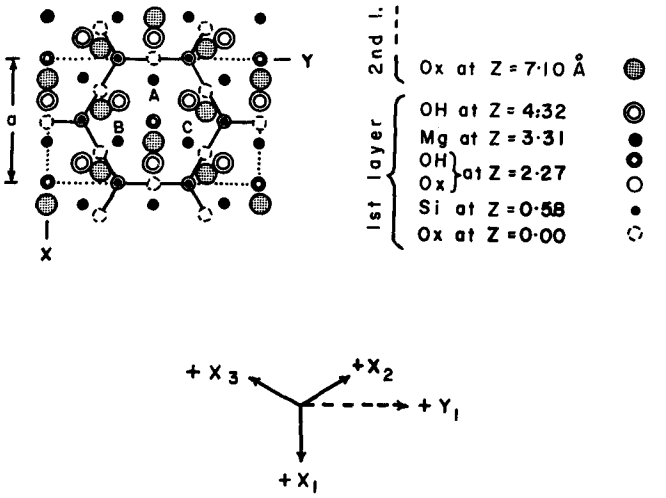

Fig. 2. Pairing of basal oxygens (stippled) with surface hydroxyls (double circles) of layer below. This orientation will be assumed for first layer of polytypes derived in Fig. 3, with the II octahedral set (3 individual sites labeled A, B, C) occupied and the second layer shifted by $a/3$ along $-X_1$.

tion of the second layer. If the layers are assumed to be undistorted, shifts along the three Y axes give identical results so that the particular Y axis used is immaterial. Interlayer shifts along the positive or negative directions of Y are both possible, regardless of the octahedral set occupied in the initial layer, but positive and negative directions of shifts lead to different resulting structures.

Variability both in the positioning of adjacent layers and in the occupancy of octahedral sets within each layer (equivalent to layer rotations) lead to different permissible stacking sequences of layers. If the three types of relative layer positioning listed above are not intermixed in the same crystal, it can be shown that there are 12 different trioctahedral 1:1 type polytypes, plus 4 enantiomorphs, with periodicities between one and six layers. This compares with 6 simple mica polytypes of similar periodicities and several hundred for the chlorites.

Interlayer shifts along X

In what follows it will be assumed that the II octahedral set of cations is always occupied in the initial layer, and that the second layer is always shifted by $a/3$ along $-X_1$ (as illustrated and defined in Fig. 2). Succeeding interlayer shifts may take any of six directions relative to this initial shift ($\pm X_1$, $\pm X_2$, $\pm X_3$). In order to depict the possible layer sequences graphically, it is convenient to modify the procedure of Smith and Yoder (1956) and to show the interlayer shifts as vectors directed from the center of a hexagonal ring in the tetrahedral sheet of a lower layer to the center of a hexagonal ring in the layer above and having a projected length of $a/3$ on (001). The interlayer stacking angle will be defined as the angle between two adjacent interlayer vectors, as measured in a counterclockwise direction in projection on (001). The six possible interlayer stacking angles are 0°, 60°, 120°, 180°, 240°, and 300°. Because of the plane of symmetry that is parallel to the interlayer shift vector, angles 60° and 300° are equivalent, as are angles 120° and 240°.

Readers familiar with mica polytypes will recognize that with interlayer shifts of $\pm a/3$ and a restriction on intermixing of interlayer stacking angles, only the six vector patterns that are possible for micas can be derived for 1:1 type layers as well. These six possibilities are illustrated graphically in Fig. 3. It is convenient to assign the same structural symbols to these 1:1 polytypes as were used for the micas. It is for this reason that the writer previously (1963) had argued against applying the $2M_1$ and $2M_2$ symbols to dickite and nacrite, which do not have the particular stacking sequences that these symbols represent for the micas. It should be noted that the resulting space groups and β angles differ for the 1:1 and 2:1 polytypes of the same structural symbol because of the differences in centrosymmetry and thickness of the corresponding layers.

In Fig. 3 the structure with 0° interlayer stacking angle, corresponding to successive $-X_1$ shifts, is the $1M$ polytype. The $2Or$ polytype results from 180° stacking angles, equivalent to alternate $-X_1$ and $+X_1$ shifts. These are the only polytypes that involve shifts along just one axis. If shifts are considered along two different X axes, then a continuous alternation of $\pm 120°$ stacking angles gives rise to the $2M_1$ polytype and a continuous alternation of $\pm 60°$ angles to the $2M_2$ polytype. Note that the fixed axes and unit cell (dashed lines) used to derive these theoretical structures are not the best axes to use for the resultant structure (solid lines). Also, in the $2M_2$ structure the X and Y axes must be reversed because the (010) symmetry plane is normal to the 5·2 Å repeat axis. Although only the X_1 and X_2 shift directions are shown in Fig. 3, any two X axes could be used. The same two structures would be derived, differing only in the orientation of the resultant unit cell relative to the fixed starting axes. Finally, if all three X axes are used for shift directions a continuous sequence of 120° angles along $-X_1$, $-X_2$, and $-X_3$ gives rise to the $3T$ polytype. Going around the vector triangle in the opposite direction with 240° angles simply gives a mirror image structure. In the same way continuous stacking angles of 60° or of 300° along all three axes gives two mirror image structures designated $6H$. Hexagonal-shaped P unit cells can be used for $3T$ and $6H$, instead of the monoclinic-shaped C cells necessary for the other polytypes.

In summary, two polytypes can be derived using shifts along just one X axis. A second set of two polytypes involves shifts along two axes, and a third set of two polytypes plus two enantiomorphs involves shifts along all three axes. One member of each of these three sets involves structures in which the same octahedral set is occupied in each layer, whereas for the other member the octahedral sets I and II are occupied alternately in successive layers (equivalent to layer rotations).

No interlayer shift

If the succeeding layers are directly superimposed on the initial layer without any shift, the additional polytypes designated $1T$ and $2H_1$ (Fig. 4) are generated. These differ from one another only in the octahedral cation sites occupied. In the $1T$ polytype the same set of octahedral positions is occupied in each layer, whereas in the $2H_1$ polytype there is alternation between the I and II sets in adjacent layers. Both polytypes are based on a hexagonal-shaped P unit cell.

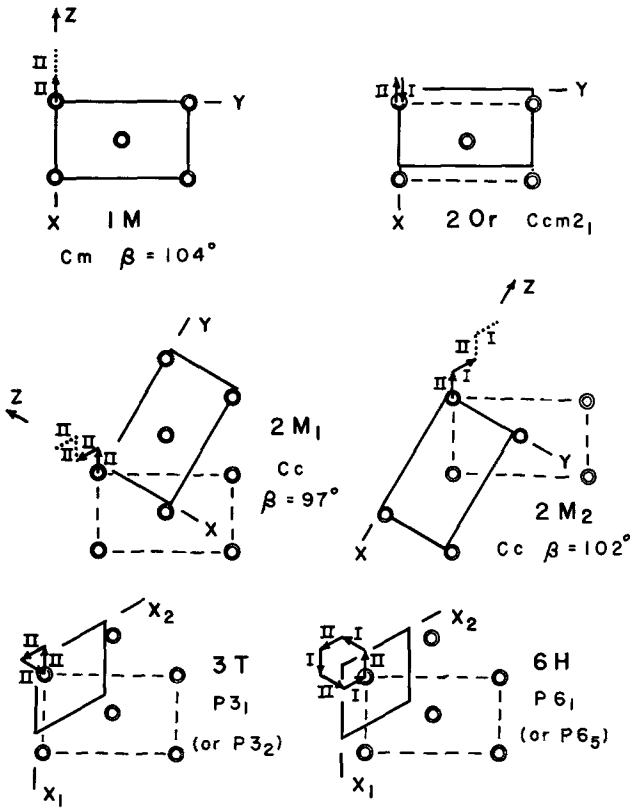

Fig. 3. Six 1:1 polytypes that result from $\pm a/3$ interlayer shifts along the three X-axes. The base of the resultant unit cell (solid lines) may or may not coincide with the fixed cell (dashed lines) used for the first layer. The origin of the resultant unit cell has been placed as close to the center of a hexagonal ring in the first layer (double circles) as the symmetry permits.

Interlayer shifts along Y

Finally, interlayer shifts of $\pm b/3$ along the Y axes lead to the four polytypes illustrated in Fig. 5. Because shifts along each Y axis lead to equivalent results, all shifts can be taken to be along Y_1. Alternating negative and positive shift directions generate the $2T$ and $2H_2$ polytypes. The same direction of shift between all layers results in the $3R$ and $6R$ polytypes. In the latter two rhombohedral cases, vectors of projected length $b/3$ end to end lead to resultant shifts of b and $2b$, which are equivalent to zero resultant shifts. As a result, all four polytypes can be shown as based on hexagonal-shaped unit cells. Both the $2H_2$ and $3R$ structures are enantiomorphic.

Comparison with other studies

Steadman (1964) assumed in his derivation of trioctahedral 1:1 polytypes that (a) interlayer displacements along X are never accompanied by rotation, and (b) although it is not permissible to intermix $\pm a/3$ shifts with $\pm b/3$ shifts or with direct superposition stacking (no shift), direct superposition can be intermixed with $\pm b/3$ shifts in the same crystal. The first assumption eliminates the $2M_2$, $2Or$, and $6H$ polytypes. The present writer prefers to retain these polytypes in order to emphasize the similarity of the stacking possibilities with those of the mica system (where these structures do occur sparingly). The second assumption introduces four new polytypes (and four enantiomorphs) that are not given in the present paper. Actually, a few natural crystals are now known in which X shifts are intermixed with no shifts and others in which Y shifts are intermixed with no shifts. There does not appear to be any justification for treating one case differently than the other. The present writer prefers to treat both as relatively

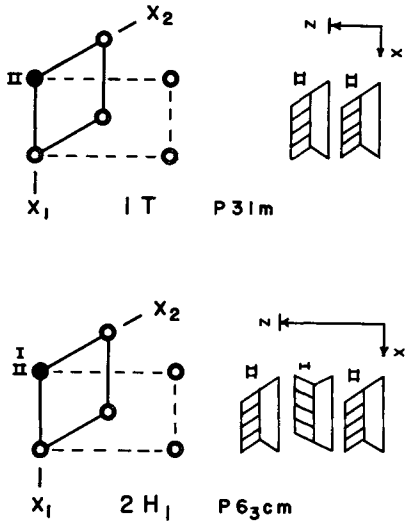

Fig. 4. Two 1:1 polytypes that result from direct superposition of layers. XZ side views illustrate the differing slants of the I and II octahedral sheets.

rare stacking variants that are exceptions to the rule of no intermixing of shift types. Steadman does not use structural symbols to designate his standard polytypes, only the space group plus a system of Greek letter and number subscripts to denote the sequence of layer displacements and rotations.

The results of the 1:1 polytype derivation by Zvyagin *et al.* (1966) and by Zvyagin (1967) are similar to that of the present writer, except that a 13th polytype labeled $2M_3$ of space group $P2_1$ is included. This appears to be a duplicate of the $2Or$ structure if only undistorted layers are considered. Zvyagin has used both structural symbols and an analytical notation system to indicate the intralayer and interlayer shifts for each polytype. The structural symbols differ from those of the present writer in the following ways.

(1) No distinction is made by Zvyagin for structures with 3-fold axes between those that are based on hexagonal-shaped P cells and those that can be indexed on rhombohedral cells. The writer uses the symbols T and R, respectively, for these cases and thereby avoids having to use the same $3T$ symbol for two different structures.

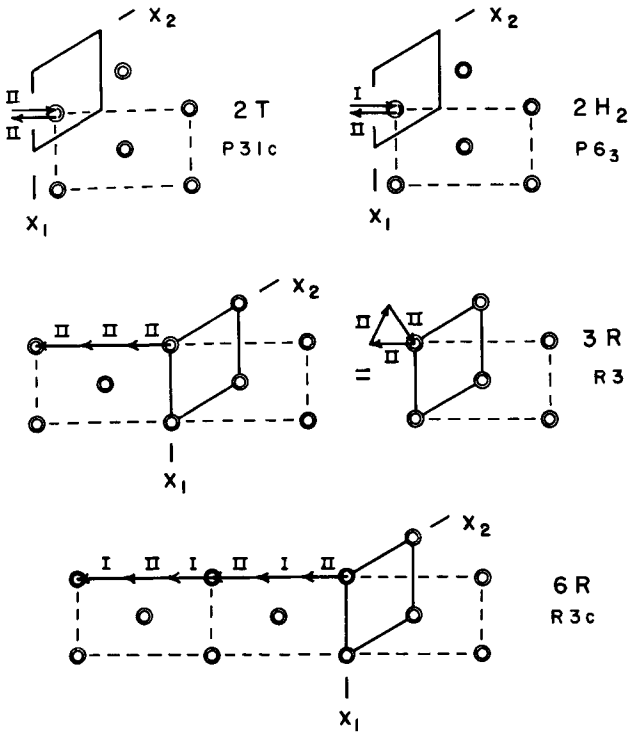

Fig. 5. Four 1:1 polytypes that result from $\pm b/3$ interlayer shifts along Y_1. Two equivalent interlayer sequences are illustrated for the $3R$ polytype.

https://doi.org/10.1346/CCMN.1969.0170605 Published online by Cambridge University Press

Table 1. Atomic coordinates as fractions of cell parameters for twelve standard polytypes

		Mg_1	Mg_2	Mg_3	Si_1	Si_2	O_1	O_2	O_3	O_4	O_5	$(OH)_1$	$(OH)_2$	$(OH)_3$	$(OH)_4$
1*T* ($P31m$)	*x*	0·667			1/3		0·500			1/3		0	0·333		
	y	0			2/3		0			2/3		0	0		
	z	0·466			0·082		0			0·320		0·320	0·608		
1*M* (Cm)	*x*	0·822	0·322		0·527		0·500	0·250		0·607		0·107	0·536	0·536	
	y	0	0·167		0·167		0	0·250		0·167		0	0	0·333	
	z	0·466	0·466		0·082		0	0		0·320		0·320	0·608	0·608	
$2M_1$ (Cc)	*x*	0·411	0·911	0·911	0·514	0·014	0·250	0·750	0	0·553	0·053	0·053	0·768	0·268	0·268
	y	0·250	0·083	0·417	0·083	0·250	0·167	0·167	0·417	0·167	0·250	0·917	0·250	0·083	0·417
	z	0·233	0·233	0·233	0·041	0·041	0	0	0	0·160	0·160	0·160	0·304	0·304	0·304
$2M_2$ (Cc)	*x*	0·078	0·411	0·245	0·347	0·181	0	0·250	0·250	0·386	0·220	0·053	0·268	0·101	0·434
	y	0·417	0·417	0·917	0·083	0·583	0·583	0·333	0·833	0·083	0·583	0·083	0·250	0·750	0·750
	z	0·233	0·233	0·233	0·041	0·041	0	0	0	0·160	0·160	0·160	0·304	0·304	0·304
2*Or* ($Ccm2_1$)	*x*	0·833	0·333		0·667		0·667	0·417		0·667		0·167	0·500	0	
	y	0	0·167		0·167		0	0·250		0·167		0	0	0·167	
	z	0·233	0·233		0·041		0	0		0·160		0·160	0·304	0·304	
2*T* ($P31c$)	*x*	0·667			0	1/3	0·167			0	1/3	2/3	0·333		
	y	0			0	2/3	0·333			0	2/3	1/3	0		
	z	0·233			0·041	0·041	0			0·160	0·160	0·160	0·304		
$2H_1$ ($P6_3cm$)	*x*	0·667			1/3		0·500			1/3		0	0·333		
	y	0			2/3		0			2/3		0	0		
	z	0·233			0·041		0			0·160		0·160	0·304		
$2H_2$ ($P6_3$)	*x*	0·667			0	1/3	0·167			0	1/3	2/3	0·333		
	y	0			0	2/3	0·333			0	2/3	1/3	0		
	z	0·233			0·041	0·041	0			0·160	0·160	0·160	0·304		
3*T* ($P3_1$)	*x*	0·889	0·556	0·222	0·889	0·556	0·722	0·722	0·222	0·889	0·556	0·222	0·556	0·889	0·222
	y	0·111	0·444	0·778	0·444	0·778	0·111	0·611	0·611	0·444	0·778	0·111	0·111	0·778	0·444
	z	0·155	0·155	0·155	0·027	0·027	0	0	0	0·107	0·107	0·107	0·203	0·203	0·203
3*R* ($R3$)	*x*	0·667			0	0	0·500			0	0	0	0·333		
	y	0			0	0	0			0	0	0	0		
	z	0·155			0·360	0·694	0			0·440	0·774	0·107	0·203		
6*H* ($P6_1$)	*x*	0·333	0·667	0	0·667	0	0·833	0·833	0·333	0·667	0	0·333	0	0·667	0·333
	y	0	0·667	0·333	0	0·667	0·333	0·833	0·833	0	0·667	0·333	0	0·333	0·667
	z	0·078	0·078	0·078	0·014	0·014	0	0	0	0·053	0·053	0·053	0·101	0·101	0·101
6*R* ($R3c$)	*x*	0·667			0·667	0·333	0·500			0·667	0·333	0	0·333		
	y	0			0·333	0·667	0			0·333	0·667	0	0		
	z	0·078			0·014	0·014	0			0·053	0·053	0·053	0·101		

(2) Zvyagin restricts usage of subscripts to monoclinic structures and uses subscripts 1, 2, and 3 with specific implication as to the orientation of symmetry elements relative to the monoclinic axes. The writer uses subscripts 1 and 2 to differentiate two $2M$ and two $2H$ structures. The subscripts are assigned in the order of derivation of the structures in the present paper with no implication as to orientation of symmetry elements.

IDENTIFICATION OF POLYTYPES

The atomic parameters of the 12 standard polytypes are listed in Table 1. Only one example of each of the four enantiomorphic pairs has been included. Structure amplitudes and powder patterns calculated from these parameters are listed in Tables 2 and 3. In the calculations identical compositions of $Mg_3Si_2O_5(OH)_4$ were assumed for all polytypes, and temperature factors of 0·8, 1·2, and 2·0 were used for Si, Mg, and (O, OH) respectively. Multiplicity and Lorentz-polarization factors were included in the powder calculations. Standard unit cell dimensions appropriate to research in progress on aluminous serpentines were used for all polytypes. These values are listed in Table 3. In natural specimens deviations from the calculated spacings and intensities are to be expected as a result of variations in composition and structural detail. Hexagonal indices *hkil* were used for all hexagonal and rhombohedral structures, but the *i* index has been omitted from the publication to conserve space.

For identification purposes the 12 polytypes can be divided into four groups (A, B, C, D), for which the strongest reflections ($k = 3n$ for monoclinic- and orthorhombic-shaped cells or *hhl* for hexagonal-shaped cells) have identical F_c values within each group but quite different values between groups. The four groups are distinguished structurally from each other either by different directions of interlayer shift or by a different occupancy pattern of octahedral cation sets. Thus, the two groups A and B (Table 2) feature interlayer shifts along X and differ in having octahedral cations in the same set in every layer ($1M$, $2M_1$, $3T$) or in alternating cations between I and II sets in adjacent layers ($2M_2$, $2Or$, $6H$). The other two groups C and D feature stacking sequences involving either no shifts or interlayer shifts along Y, which cannot be differentiated by these particular reflections. The groups differ again in having octahedral cations in the same set throughout ($1T$, $2T$, $3R$) or in alternating cations between the I and II sets ($2H_1$, $2H_2$, $6R$).

Thus, classification of a good X-ray diffraction pattern of an unknown 1 : 1 layer silicate into one of four groups can be accomplished easily by means of the most intense reflections. This immediately defines the direction of interlayer shift and the occupancy pattern of octahedral cation sets in the structure. Further differentiation between the three structures within each group must be made on the basis of the weaker reflections, which indicate the precise layer stacking sequence. These are the $k \neq 3n$ reflections for monoclinic- and orthorhombic-shaped cells and $h \neq k$ reflections (excluding $30l$)

Table 2. Structure amplitudes for strong reflections of four groups of standard polytypes

	Group A $1M$–$2M_1$–$3T$		Group B $2Or$–$2M_2$–$6H$	Group C $1T$–$2T$–$3R$	Group D $2H_1$–$2H_2$–$6R$
d (Å)	F_c	d (Å)	F_c	F_c	F_c
2·649	25	2·670	11	12	8
2·590	17	2·624	17	0	11
2·387	54	2·499	24	18+51	34
2·262	13	2·326	32	0	22
2·007	33	2·134	17	19+39	17
1·886	18	1·945	15	0	27
1·665	47	1·771	25	9+45	18
1·568	31	1·615	33	0	25
1·396	16	1·478	8	44+30	29
1·322	44	1·358	28	0	20
1·191	14	1·254	21	32+10	19
1·134	6	1·162	3	0	12

Calculations made with $B = 1·2$, 0·8, and 2·0 for Mg, Si, and O, OH respectively, and normalized to one formula unit. Indices are of type $20l$ for monoclinic and orthorhombic C cells (except $2M_2$) and $11l$ for hexagonal P cells. In group C, $F_c(11\bar{l}) \neq F_c(11l)$. Spacings are from Table 3.

Table 3. Calculated X-ray powder patterns for standard 1 : 1 polytypes

Group A						Group B						Group C		
$1M$ (= $3T$)			$2M_1$			$2M_2$ (= $6H$)			$2Or$			$1T$		
hkl	*d*(Å)	Int	*hkl*	*d*(Å)	Int	*hkl*	*d*(Å)	Int	*hkl*	*d*(Å)	Int	*hkl*	*d*(Å)	Int
001	7·100	88	002	7·100	88	002	7·100	100	002	7·100	100	001	7·100	82
020	4·625	14	020	4·625	3	110	4·598	23	020, 110	4·625	23	100	4·625	42
110	4·519	27	110	4·598	20	11$\bar{1}$, 200	4·519	22	111	4·397	40	101	3·875	46
11$\bar{1}$	4·242	22	11$\bar{1}$	4·519	6							002	3·550	57
021	3·875	17	021	4·397	18	111, 20$\bar{2}$	4·242	18	022, 112	3·875	28	102	2·816	15
002	3·550	60	111	4·242	5	11$\bar{2}$	4·064	16	004	3·550	68	110	2·670	5
111	3·492	12	11$\bar{2}$	4·064	14	112	3·682	12	113	3·308	17	111, 11$\bar{1}$	2·499	100
11$\bar{2}$	3·133	8	022	3·875	4	004	3·550	68	024, 114	2·816	10	003	2·367	6
022	2·816	6	112	3·682	11	11$\bar{3}$, 202	3·492	10	200	2·670	6	200	2·312	1
20$\bar{1}$	2·649	26	004	3·550	60				201	2·624	27	201	2·199	3
200	2·590	12	11$\bar{3}$	3·492	3	113, 20$\bar{4}$	3·133	7	202	2·499	51	112, 11$\bar{2}$	2·133	45
112	2·542	4	023	3·308	7	11$\bar{4}$	2·969	6	115	2·420	5			
20$\bar{2}$	2·387	100	113	3·133	2	114	2·673	4	006	2·367	7	103	2·107	5
003	2·367	6	11$\bar{4}$	2·969	5	020	2·670	6	203	2·326	78	202	1·938	5
11$\bar{3}$	2·307	3	114	2·674	3	021	2·624	27	042, 222	2·199	2	004	1·775	1
201	2·263	6	200	2·649	26	11$\bar{5}$, 204	2·542	3	204	2·134	18	113, 11$\bar{3}$	1·771	32
023	2·107	2	20$\bar{2}$	2·590	12	022	2·499	51	026, 116	2·107	3	120	1·748	4
221	2·032	2	025	2·420	2	006	2·367	7						
20$\bar{3}$	2·007	25	202	2·387	100	023	2·326	78	223	2·078	2	121	1·697	7
042	1·938	2	006	2·367	6	115, 206	2·307	2	205	1·945	10	203	1·654	4
202	1·886	6	20$\bar{4}$	2·262	6	11$\bar{6}$	2·203	2	044, 224	1·938	3	122	1·568	5
22$\bar{3}$	1·841	2	204	2·007	25	024	2·134	18	225	1·793	3	300	1·542	26
004	1·775	1	20$\bar{6}$	1·885	6	025	1·945	10	008	1·775	1	301	1·506	11
222	1·746	2	008	1·775	1	008	1·775	1	206	1·771	24	114, 11$\bar{4}$	1·478	28
150	1·742	3	150	1·746	3	026	1·771	24	150, 310	1·748	3	005	1·420	2
15$\bar{1}$	1·725	3	310	1·735	2	42$\bar{1}$, 404	1·746	4	151	1·735	5	302	1·414	6
31$\bar{2}$	1·697	2	15$\bar{2}$	1·712	2	42$\bar{2}$, 13$\bar{1}$	1·742	2	152, 312	1·697	4	204	1·408	3
20$\bar{4}$	1·665	32	152	1·680	2							123	1·406	2
151	1·661	2	206	1·665	32	131, 420	1·725	2	046, 226	1·654	3	220	1·335	3
15$\bar{2}$	1·617	2	312	1·640	2									

https://doi.org/10.1346/CCMN.1969.0170605 Published online by Cambridge University Press

Table 3. (*contd.*)

Group C (*cont.*)						Group D							
	2*T*			3*R*			2H_1			2H_2			6*R*	
hkl	*d*(Å)	Int	*hkl*	*d*(Å)	Int	*hkl*	*d*(Å)	Int	*hkl*	*d*(Å)	Int	*hkl*	*d*(Å)	Int
002	7·100	82	003	7·100	82	002	7·100	100	002	7·100	100	006	7·100	100
100	4·624	11	101	4·519	36	100	4·625	45	100	4·625	13	$10\bar{2}$	4·519	42
101	4·397	53	$10\bar{2}$	4·242	30	102	3·875	55	101	4·397	64	104	4·242	35
102	3·875	12	006	3·550	57	004	3·550	68	102	3·875	14	0, 0, 12	3·550	68
004	3·550	57	104	3·492	17	104	2·816	19	004	3·550	68	$10\bar{8}$	3·492	20
103	3·308	22	$10\bar{5}$	3·133	12	110	2·670	3	103	3·308	27	1, 0, 10	3·133	14
104	2·816	4	110	2·670	5	111	2·624	12	104	2·816	5	110	2·670	3
110	2·670	5	107	2·542	5	112	2·499	98	110	2·670	3	113	2·624	12
112, $11\bar{2}$	2·499	100	$11\bar{3}$, 113	2·499	100	006	2·367	7	111	2·624	12	1, 0, $\overline{14}$	2·542	6
105	2·420	6	009	2·367	6	113	2·326	35	112	2·499	98	116	2·499	98
006	2·367	6	$10\bar{8}$	2·307	4	200	2·312	1	105	2·420	8	0, 0, 18	2·367	7
201	2·282	2	$11\bar{6}$, 116	2·133	45	202	2·199	4	006	2·367	7	119	2·326	35
202	2·199	1				114	2·134	17	113	2·326	35	1, 0, 16	2·307	4
114, $11\bar{4}$	2·133	45	$20\bar{4}$	2·121	2	106	2·107	5	201	2·282	2	$20\bar{4}$	2·260	2
			205	2·032	2	115	1·945	35	114	2·134	17	1, 1, 12	2·134	17
106	2·107	1	$20\bar{7}$	1·841	2	204	1·938	5	203	2·078	4	208	2·121	2
203	2·078	3	0, 0, 12	1·775	1	008	1·775	1	115	1·945	35	2, 0, $\overline{10}$	2·032	3
204	1·938	1	$11\bar{9}$, 119	1·771	32	116	1·771	12	107	1·858	2	1, 1, 15	1·945	35
			208	1·746	2	120	1·748	5	205	1·793	4	1, 0, $\overline{20}$	1·935	2
107	1·858	2	$12\bar{1}$	1·742	4	122	1·697	9	008	1·775	1	2, 0, 14	1·841	3
205	1·793	3	122	1·725	4	108	1·657	2	116	1·771	12	0, 0, 24	1·775	1
008	1·775	1	$12\bar{4}$	1·661	3	206	1·654	5	121	1·735	7	1, 1, 18	1·771	12
116, $11\bar{6}$	1·771	32	125	1·617	3	117	1·615	20	122	1·697	2	2, 0, $\overline{16}$	1·746	3
			2, 0, $\overline{10}$	1·567	2	124	1·568	5	123	1·640	5	$21\bar{2}$	1·742	5
121	1·735	6	300	1·542	26	300	1·542	33	117	1·615	20	214	1·725	5
122	1·697	2	$12\bar{7}$	1·516	2	302	1·506	14	300	1·542	33	$21\bar{8}$	1·661	4
123	1·640	4	303	1·506	11	118	1·478	21	207	1·525	3	2, 1, 10	1·617	3
300	1·542	26	2, 0, 11	1·485	2	0, 0, 10	1·420	2	302	1·506	14	1, 1, 21	1·615	20
207	1·525	3				304	1·414	8	125	1·489	3	2, 0, 20	1·567	2
302	1·506	11	1, 1, $\overline{12}$, 1, 1, 12	1·478	28	208	1·408	4	118	1·478	21	300	1·542	55
125	1·489	2	0, 0, 15	1·420	2	126	1·406	3	0, 0, 10	1·420	2	2, 1, $\overline{14}$	1·516	2

https://doi.org/10.1346/CCMN.1969.0170605 Published online by Cambridge University Press

Table 3. (*contd.*)

Group A					Group B						Group C			
	1M (= 3*T*)			2*M*$_1$		2*M*$_2$ (= 6*H*)			2*Or*			1*T*		
hkl	d(Å)	Int	*hkl*	*d*(Å)	Int	*hkl*	d(Å)	Int	*hkl*	*d*(Å)	Int	*hkl*	*d*(Å)	Int
$31\bar{3}$ / 203	1·568	14	$20\bar{8}$	1·568	14	$42\bar{3}$	1·712	2	153	1·640	4	221 / $22\bar{1}$	1·312	15
060	1·542	29	060	1·542	29	421	1·680	2	207	1·615	34	303	1·292	4
061	1·506	13	062	1·506	13	$13\bar{3}$	1·661	2	154 / 314	1·568	3	130	1·283	1
005	1·420	2	0, 0, 10	1·420	2	133	1·617	2	060	1·542	33	131	1·262	2
062	1·414	7	064	1·414	7	027	1·615	34	227	1·525	2	115 / $11\bar{5}$	1·254	8
$20\bar{5}$	1·396	3	208	1·396	3	$60\bar{2}$	1·542	33	062	1·506	14	222 / $22\bar{2}$	1·250	4
$40\bar{1}$	1·332	7	$40\bar{2}$	1·332	7	600	1·506	14	155	1·489	2	124	1·245	1
$40\bar{2}$	1·325	3	2, 0, $\bar{1}0$	1·322	16	028	1·478	2	208	1·478	2	205	1·210	2
204	1·322	16	400	1·304	3	0, 0, 10	1·420	2	0, 0, 10	1·420	2	006	1·183	1
400	1·295	9	$40\bar{4}$	1·295	9	602	1·414	7	064	1·414	7			
063	1·292	4	066	1·292	4	029	1·358	16	048	1·408	2	223 / $22\bar{3}$	1·163	7
			402	1·274	4	040	1·335	2	209	1·358	16			

Calculations of I = LpmF^2 made using $Mg_3Si_2O_5(OH)_4$ compositions and cell parameters of $a = 5{\cdot}340$, $b = 9{\cdot}249$, $c \sin\beta = 7{\cdot}100$ A with β values of 104°04′ (1*M*), 97°09′ (2*M*$_1$), and 102°15′ (2*M*$_2$). Hexagonal indices *hkil* used for both hexagonal and rhombohedral symmetries, but *i* index omitted here to conserve space.

for hexagonal-shaped cells. If these reflections are streaked out due to stacking disorder, the three structures within each group are indistinguishable but the four groups are still evident from the stronger non-streaked reflections.

Group *A* (1*M*, 2*M*$_1$, 3*T*) differs from the three other groups in the *d*-values of its strongest reflections. As in the micas, the 1:1 trioctahedral 1*M* and 3*T* X-ray powder patterns are identical so that differentiation of these two must be made by single crystal determination. The 2*M*$_1$ powder pattern can be recognized both by additional weak reflections not present in the 1*M* and 3*T* patterns and by a different ratio of *hkl* ($k \neq 3n$) to 00*l* intensities due to multiplicity differences.

In group *B* (2*M*$_2$, 2*Or*, 6*H*) the powder patterns of the 2*M*$_2$ and 6*H* polytypes are also identical, as in the micas, and single crystal study is needed for differentiation. The 2*Or* pattern can be recognized because it has $k \neq 3n$ reflections that are fewer in number and occur at different *d*-values than for the 2*M*$_2$ and 6*H* patterns.

In group *C* (1*T*, 2*T*, 3*R*) about one-half of the weak $h \neq k$ reflections are similar for the 1*T* and 2*T* patterns but the 2*T* pattern has additional weak reflections that verify its 2-layer nature. The 3*R* weak reflections have different *d*-values than for 1*T* and 2*T*. A similar situation exists in group *D* (2*H*$_1$, 2*H*$_2$, 6*R*), in which there are additional weak reflections for 2*H*$_2$ that differentiate it from the otherwise similar pattern of 2*H*$_1$. The 6*R* pattern has *d*-values for its weak reflections that are different from those of the 2*H*$_1$ and 2*H*$_2$ patterns.

NATURAL EXAMPLES

The data in Tables 1–3 permit correlation of natural 1:1 layer silicates with the theoretical stacking sequences derived in this paper. Examples of all four major groups are known to exist in nature and definite correlations can be made with at least nine of the twelve individual structures. Table 4 lists the correlations that have been made to date, including the dioctahedral analogues. Several minerals have been classified only as to Groups *A*–*D* because of the absence of the weak reflections that specify the exact layer sequences. There is a strong tendency for certain compositions to prefer specific stacking sequences so that most natural specimens are neither polytypic nor polymorphic with one another. An exception to this generaliza-

Table 3. (*contd.*)

Group C (*cont.*)														
	2*T*			3*R*			2H_1			2H_2			6*R*	
hkl	*d*(Å)	Int	*hkl*	*d*(Å)	Int	*hkl*	*d*(Å)	Int	*hkl*	*d*(Å)	Int	*hkl*	*d*(Å)	Int
11$\bar{8}$ / 118	1·478	28	306	1·414	6	119	1·358	8	304	1·414	8	306	1·506	14
			220	1·335	3									
0, 0, 10	1·420	2	22$\bar{3}$ / 223	1·312	15	1, 0, 10	1·357	1	119	1·358	8	2, 0, $\bar{22}$	1·485	2
304	1·414	6				220	1·335	3	220	1·335	3	1, 1, 24	1·478	21
220	1·335	3	309	1·292	4	221	1·329	2	221	1·329	2	2, 1, 16	1·461	2
222 / 22$\bar{2}$	1·312	15	1, 1, $\bar{15}$ / 1, 1, 15	1·254	8	222	1·312	16	222	1·312	16	0, 0, 30	1·420	2
209	1·303	2	22$\bar{6}$ / 226	1·250	4	306	1·292	4	209	1·303	2	3, 0, 12	1·414	8
306	1·292	4				223	1·285	3	306	1·292	4	1, 1, 27	1·358	8
			0, 0, 18	1·183	1									
131	1·277	2				130	1·283	1	223	1·285	3	2, 0, 26	1·337	2
			22$\bar{9}$ / 229	1·162	7	132	1·262	3	131	1·277	2	220	1·335	3
1, 1, 10 / 1, 1, $\bar{10}$	1·254	8												
						1, 1, 10	1·254	6	1, 1, 10	1·254	6	223	1·329	2
224 / 22$\bar{4}$	1·250	4				2, 0, 10	1·210	2	133	1·238	2	226	1·312	16
0, 0, 12	1·183	1				225	1·208	4	225	1·208	4	3, 0, 18	1·292	4

tion may be the mineral cronstedtite, in which Steadman and Nuttall (1963, 1964) have confirmed a large number of different stacking arrangements from crystals of *apparently* similar compositions.

Aluminous serpentines also show several different stacking arrangements, although for different compositions. In addition to 1*T* lizardite, which extends into the Al-rich compositions, and amesite (2H_2+2H_1) there are several unnamed species. The type *F* aluminous serpentine of Bailey and Tyler (1960) can be correlated with the 1*M*–3*T* powder pattern of Table 3. Jahanbagloo and Zoltai (1968), however, have shown that single crystals of material that gives the same powder pattern as type *F* must really be 9-layer or 18-layer structures in order to explain all of the weak reflections. Their proposed structure intermixes shifts along X with direct superposition of layers. Steadman and Nuttall (1962, 1963) have found one specimen of amesite and one of cronstedtite that contain crystals that have a complex 6-layer structure intermixing shifts along Y with direct superposition of layers.

Table 4. Natural examples of 1 : 1 structures

Trioctahedral		Dioctahedral	
Lizardite	1*T*	kaolinite	1*Tc* = [1M_{ord}]
Antigorite	~ 1*T*	dickite	2*M* = [1M_{ord}]
Clinochrysotile	~ 1*T* (+ ~ 1*M* rare?)		
Orthochrysotile	~ 2*Or*	nacrite	2*M* = [6R_{ord}]
Al-serpentine	1*T*, 1*M*–3*T*		
Amesite	2H_2 (+ 2H_1 rare)		
Berthierine (= 1 : 1 chamosite)	1*T*, 1*M*–3*T*		
Cronstedtite	1*T*, 3*T*, 2H_1, 2H_2, 2*T*, 1*M*, 2M_1		
Greenalite	group *C*		
Garnierite	group *C*		

https://doi.org/10.1346/CCMN.1969.0170605 Published online by Cambridge University Press

The Unst 6-layer aluminous serpentine of Brindley and von Knorring (1954) also must be a complex stacking variant. Its strongest reflections fit well those of group D ($2H_1, 2H_2, 6R$) of Table 2, but the weaker reflections do not fit. The structure must involve shifts along Y and alternation of the I and II octahedral cation sets. A further publication is planned on the complex stacking variants found in aluminous serpentines.

It is interesting to note that the magnesian serpentines lizardite, antigorite, and clinochrysotile are all based on the $1T$ structure, or on modifications of the $1T$ structure. The massive, platy variety lizardite is mainly $1T$, although stacking faults make some specimens transitional between $1T$ and $2H_1$. Antigorite is basically a $1T$ structure also, but with a regular, wave-like inversion of tetrahedra that distorts the geometry so that the β angle (91°23′) is not exactly 90°. The $1T$ structure is distorted still further in clinochrysotile as a result of its cylindrical fibre morphology. In most fibres the X-axis is parallel to the fibre length, and the individual layers are out of register with one another along the cylindrical Y-axis because of the progressive change in cylinder radius from layer to layer. In the structure determination by Whittaker (1956*a*) adjacent layers are shifted along $+X_1$, as defined in Fig. 2, by a regular small amount (about $a/13$ to give $\beta = 93°16'$). This shifts the basal oxygens slightly away from the optimum superposition arrangement in the $1T$ structure so that only 2/3 of the basal oxygens can be described as having hydrogen bond contacts. The remaining 1/3 lie over niches in the hydroxyl surface below, presumably to anchor the layers within the cylindrical helix. The strong reflections can be correlated with those of group C, after making allowance for the separation of $11\bar{l}$ and $11l$ reflections resulting from the monoclinic geometry. Some specimens show 2-layer periodicity due to small distortions of $\pm 0{\cdot}019a$ that alternate in direction in adjacent layers.

In contrast to the small interlayer shift of $0{\cdot}078a$ in clinochrysotile, Whittaker (1956*b*) reports alternating interlayer shifts of $\pm 0{\cdot}441a$ along X_1 for cylindrical fibres of orthochrysotile, plus regular alternation of I and II octahedral cation sets in adjacent layers. Thus, the orthochrysotile structure is a distortion of the $2Or$ structure, for which the ideal interlayer shifts should be $\pm 0{\cdot}333a$ along X_1. The observed "overshift" of $0{\cdot}108a$ is analogous to the distortional shifts of $0{\cdot}078a$ found in the $\sim 1T$ clinochrysotile structure. In orthochrysotile the "overshift" leads to exactly the same anchoring relationship of the basal oxygens relative to the hydroxyl surface within the cylindrical fibres as is observed in clinochrysotile. It should be noted that this structure (group B) could not be identified from the four groups of Table 2, because the strong reflections fit best those of group D (which implies no shift along X). This is because the observed shift of $0{\cdot}441a$ is close to $a/2$, and reflections of index $20l$ do not differentiate between shifts of 0 or $a/2$ along X.

The clinochrysotile structure described by Whittaker (1956*a*) is not related to the $1M$ or $2M_1$ structures, as the interlayer shift is both too small and in the wrong direction. There does not appear to be any reason, however, why a distorted $1M$ clinochrysotile should not occur in nature to a limited extent. A $1M$ structure with an "overshift" along $-X_1$ by an amount similar to that observed in orthochrysotile would lead to a β angle of about 107° and a similar anchored arrangement of layers within the cylindrical surface. Shitov and Zvyagin (1966) have described three clinochrysotile specimens with β angles near 107° that may correspond to this $\sim 1M$ structure. The relative stability and abundance (see next section) of the $\sim 1M$ chrysotile should be intermediate between those of the $\sim 1T$ and $\sim 2Or$ chrysotiles. The strong reflections of the $\sim 1T$ and $\sim 1M$ clinochrysotiles presumably would be quite similar in intensity because $20l$ reflections do not distinguish between interlayer shifts near $+1/12a$ and near $-5/12a$. From a consideration of the relative stabilities one would also predict a second form of orthochrysotile based on a distorted $2H_1$ structure, which theoretically should be more abundant than the observed $\sim 2Or$ structure. The strong reflections of a $\sim 2H_1$ structure, which would no longer be truly hexagonal, would belong to group D and would, as a result, be difficult to distinguish from those of the $\sim 2Or$ structure.

The Ni-serpentine garnierite and the Fe-serpentine greenalite appear to fit best into group C, according to the data summarized by Brindley (1961). The specimens examined to date are poorly crystallized, and their powder patterns do not exhibit any of the weaker reflections needed to classify them in more detail. On the other hand the Fe-rich berthierines, termed 1:1 chamosites in some of the earlier literature (e.g. Brindley, 1951), give more complete powder patterns but with some line broadening due to small particle size. The hexagonal form can be identified as the $1T$ structure, and the monoclinic form as the $1M$ or $3T$ structure.

DIOCTAHEDRAL ANALOGUES

Table 4 includes the dioctahedral kaolin minerals, but these require special comment. Previous polytype derivations for trioctahedral micas (Smith and Yoder, 1956) and for trioctahedral chlorites (Bailey and Brown, 1962) were found to apply without change to the dioctahedral species as well. There

were no changes in the space groups or layer periodicities in these mineral groups because of the location of the vacant octahedral site.

For all three kaolin minerals, however, the location of the vacant octahedral site changes the space groups from those of the corresponding trioctahedral 1:1 structures and changes the layer periodicity for two of the three. Bailey (1963) has pointed out previously that kaolinite and dickite are both based on the $1M$ stacking sequence and would be identical if they were trioctahedral. In kaolinite the vacant site is the same in each layer, at position C in Fig. 2 (or at the mirror image position B). This imposes triclinic symmetry on the structure due to loss of the symmetry planes that relate B to C. The structure is also distorted slightly to triclinic geometry (Brindley and Robinson, 1946). In dickite the vacant site alternates regularly between C and B in successive layers to create a 2-layer monoclinic structure. In nacrite the sequence of layers is that of the $6R$ polytype. The pattern of vacant sites causes the loss of the three-fold axes, which reduces the symmetry to monoclinic and allows selection of an inclined Z axis that has true two-layer periodicity. The conventional X and Y axes must be reversed in the structure, for the same reason as in the $2M_2$ structure. The symbols in brackets in Table 4 are used to indicate that the observed periodicities and symmetries for these three minerals are a result of vacant site ordering within the ideal stacking sequences that are listed in the brackets.

RELATIVE STRUCTURAL STABILITIES

It should be possible to predict something about the relative structural stabilities of the 1:1 standard polytypes by considering the relative amounts of attraction and repulsion between the ions in the structures, as was discussed by Newnham (1961) in relation to the dioctahedral minerals. Different stacking sequences lead to different patterns of superposition of ions in adjacent layers and, therefore, to different amounts of attraction and repulsion.

Bailey and Brown (1962) and Shirozu and Bailey (1965) found the presence or absence of repulsion between tetrahedral and octahedral cations to be an important structural factor in the stability of chlorite minerals. They were concerned in the case of chlorites with octahedral cations in the interlayer sheet relative to tetrahedral sheets on both sides. In 1:1 layer silicates the analogous situation refers to tetrahedral cation positions in one layer relative to octahedral positions in the layer below. The layer sequences for the 1:1 standard polytypes result in minimum tetrahedral-octahedral repulsion for all structures in groups C and D (Table 2) and maximum repulsion for all those in groups A and B. In the latter groups the octahedral and tetrahedral cations exactly superimpose.

The direction of tetrahedral rotation in response to tetrahedral–octahedral lateral misfit is a second important structural factor. Bailey (1966) has analyzed the forces that determine the rotational direction for trioctahedral 1:1 layer silicates and has ranked these in terms of the strength of their influence on the basal tetrahedral oxygens, as follows.

(1) Attraction of basal oxygens by octahedral cations in the layer immediately below.

(2) Attraction of basal oxygens by hydroxyl groups in layer below. The oxygens move to shorten the interlayer OH—O bonds.

(3) Attraction of basal oxygens by octahedral cations in same layer.

For different layer sequences each of these forces may act either in unison with or in opposition to any of the other forces, but (1) has such a strong influence that it alone can determine the rotation direction even in opposition to both of the other forces. Assuming the criteria above to be valid, the direction of probably tetrahedral rotation in the standard 1:1 polytypes can be predicted. Based only on the interaction of these forces in each structure, the predicted order of structural stability for the four groups is $C > D > A > B$.

The third factor that is considered in this paper is additional repulsion between cations that are separated by greater distances, as follows.

(1) Repulsion between tetrahedral cations of adjacent layers.

(2) Repulsion between octahedral cations of adjacent layers.

(3) Repulsion between tetrahedral cations in one layer and octahedral cations in the layer above, or vice-versa.

Table 5 summarizes the results of all three structural factors that have been considered. Each has been weighted according to the writer's best judgment as to its relative importance, based primarily on the charges on the ions involved and the distances over which the forces must be effective. The final result is a stability index for each structure that takes into account both the favorable and unfavorable structural features. The resultant order of relative structural stability is (1) group C, (2) group D, (3) group A, and (4) group B.

The predicted relative structural stabilities of the four groups are in moderately good agreement with the relative abundances of the structures in nature, as listed in Table 4. Group C, especially structure $1T$, is very common, groups D and A are intermedi-

Table 5. Summation of structural factors that influence stability. Features that cause repulsion or weakening of a bond marked by (−), strengthening of a bond by (+)

Feature	Relative weight	Group A $1M = 2M_1 = 3T$	Group B $2M_2 = 2Or = 6H$	Group C $1T$	Group C $2T = 3R$	Group D $2H_1$	Group D $2H_2 = 6R$
Repulsion tet. cations and oct. cations below	5	−	−				
Tetrahedral rotation: to lower oct. cation	5	0	0	+	+	+	+
Tetrahedral rotation: to shorten OH—O bond	2	+	+	−	−	−	−
Tetrahedral rotation: to upper oct. cation	2	+	−	+	+	−	−
Repulsion tet. cations of adjacent layers	½			−	½−	−	½−
Repulsion oct. cations of adjacent layers	½			−	−		
Repulsion tet. cations and oct. cations in layer above.	¼		−				
Stability index		$\frac{4+}{5-} = 0{\cdot}80$	$\frac{2+}{7{\cdot}25-} = 0{\cdot}28$	$\frac{7+}{3-} = 2{\cdot}33$	$\frac{7+}{2{\cdot}75-} = 2{\cdot}55$	$\frac{5+}{4{\cdot}5-} = 1{\cdot}11$	$\frac{5+}{4{\cdot}25-} = 1{\cdot}18$

ate in abundance, and group *B* is represented only by the distorted orthochrysotile structure ~ 2*Or*. Two of the three standard 1 : 1 structures that have not been identified ($2M_2$ and $6H$) belong to the least favorable structural group. It is disturbing to note in most cases, however, that the criteria used do not distinguish adequately between the individual structures within each group. The $3R$ structure would appear to be expecially favorable, yet it has not been identified in nature for certain. Both Hendricks (1939*b*) and Frondel (1962) have described $3R$ cronstedtite, but a more detailed analysis by Steadman and Nuttall (1963) suggests instead that this is the $3T$ structure of space group $P3_1$.

Evidently additional criteria are necessary to correlate the individual structures (rather than the four groups of structures) with their probability of adoption in nature. Among the non-structural factors that undoubtedly are important also are temperature and rate of crystallization, growth mechanism, pressure, solution chemistry, and composition. The preference of certain compositions for specific layer sequences is especially impressive (Table 4).

Acknowledgments—This study was supported in part by the University of Wisconsin Research Committee, in part by Petroleum Research Fund grant No. 1176-A2, administered by the American Chemical Society, and in part by National Science Foundation grants GP-4843 and GA-1681. Use of the University of Wisconsin Computing Center was made possible through support, in part, from the National Science Foundation, other United States Government agencies, and the Wisconsin Alumni Research Foundation (WARF) through the University of Wisconsin Research Committee. The writer expresses his appreciation to Carol W. Miller for assistance in the polytype derivation and to Dr. J. J. Finney and Dr. R. A. Eggleton for computational assistance.

REFERENCES

Bailey, S. W. (1963) Polymorphism of the kaolin minerals: *Am. Mineralogist* **48**, 1196–1209.

Bailey, S. W. (1966) The status of clay mineral structures: *Clays and Clay Minerals* **14**, 1–23.

Bailey, S. W. (1967) Polytypism of layer silicates: *Am. Geol. Inst. Short Course Lecture Notes*, New Orleans, SB1-27A.

Bailey, S. W., and Brown, B. E. (1962) Chlorite polytypism—I. Regular and semi-random one-layer structures: *Am. Mineralogist* **47**, 819–850.

Bailey, S. W., and Tyler, S. A. (1960) Clay minerals associated with the Lake Superior iron ores: *Econ. Geol.* **55**, 150–175.

Brindley, G. W. (1951) The crystal structure of some chamosite minerals: *Mineral. Mag.* **29**, 502–525.

Brindley, G. W. (1961) Kaolin, serpentine, and kindred minerals, In *The X-ray Identification and Crystal Structures of Clay Minerals*: (Edited by G. Brown), Chap. 2, pp. 51–131. Mineralogical Soc. (London).

Brindley, G. W., and Robinson, Keith (1946) The structure of kaolinite: *Mineral. Mag.* **27**, 242–253.

Brindley, G. W., and von Knorring, O. (1954) A new variety of antigorite (ortho-antigorite) from Unst, Shetland Islands: *Am. Mineralogist* **39**, 794–804.

Frondel, Clifford (1962) Polytypism in cronstedtite: *Am. Mineralogist* **47**, 781–783.

Gruner, John W. (1932) The structure of dickite: *Z. Krist.* **83**, 394–404.

Hendricks, Sterling B. (1939*a*) The crystal structure of nacrite $Al_2O_3 \cdot 2SiO_2 \cdot 2H_2O$ and the polymorphism of the kaolin minerals: *Z. Krist.* **100**, 509–518.

Hendricks, Sterling B. (1939*b*) Random structures of layer minerals as illustrated by cronstedtite ($2FeO \cdot Fe_2O_3 \cdot SiO_2 \cdot 2H_2O$). Possible iron content of kaolin: *Am. Mineralogist* **24**, 529–539.

Jahanbagloo, I. Cyrus, and Zoltai, Tibor (1968) The crystal structure of a hexagonal Al-serpentine: *Am. Mineralogist* **53**, 14–24.

Newnham, Robert E. (1961) A refinement of the dickite structure and some remarks on polymorphism in kaolin minerals: *Mineral. Mag.* **32**, 683–704.

Shirozu, Haruo, and Bailey, S. W. (1965) Chlorite polytypism—III: Crystal structure of an orthohexagonal iron chlorite: *Am. Mineralogist* **50**, 868–885.

Shitov, V. A., and Zvyagin, B. B. (1966) Electron microdiffraction study of serpentine minerals: *Soviet Physics-Cryst.* (*Engl. transl.*) **10**, 711–716.

Smith, J. V., and Yoder, H. S. (1956) Experimental and theoretical studies of the mica polymorphs: *Mineral. Mag.* **31**, 209–235.

Steadman, R. (1964) The structures of trioctahedral kaolin-type silicates: *Acta Cryst.* **17**, 924–927.

Steadman, R., and Nuttall, P. M. (1962) The crystal structure of amesite: *Acta Cryst.* **15**, 510–511.

Steadman, R., and Nuttall, P. M. (1963) Polymorphism in cronstedtite: *Acta Cryst.* **16**, 1–8.

Steadman, R., and Nuttall, P. M. (1964) Further polymorphism in cronstedtite: *Acta Cryst.* **17**, 404–406.

Whittaker, E. J. W. (1956*a*) The structure of chrysotile—II. Clinochrysotile: *Acta Cryst.* **9**, 855–862.

Whittaker, E. J. W. (1956*b*) The structure of chrysotile—III. Orthochrysotile: *Acta Cryst.* **9**, 862–864.

Zvyagin, B. B. (1962) Polymorphism of double-layer minerals of the kaolinite type: *Soviet Physics-Cryst.* (*Engl. transl.*) **7**, 38–51.

Zvyagin, B. B. (1967) *Electron Diffraction Analysis of Clay Minerals*: New York, Plenum Press, 364 pp.

Zvyagin, B. B., Mischenko, K. S., and Shitov, V. A. (1966) Ordered and disordered polymorphic varieties of serpentine type minerals, and their diagnosis: *Soviet Physics-Cryst.* (*Engl. transl.*) **10**, 539–546.

Résumé—Le polytypisme des phyllosilicates 1 : 1 trioctahédriques résulte de deux caractéristiques variables de la structure. (1) Les cations octahédriques peuvent occuper le même arrangement de trois positions ou peuvent changer régulièrement entre deux arrangements différents des positions dans des couches successives. (2) La liaison d'hydrogène entre les surfaces adjacentes d'oxygène

et d'hydroxyl des couches successives, peut être obtenu en partant de trois positions relatives différentes des couches: (a) superposition directe des couches, (b) déplacement de la deuxième couche par $a/3$ le long de l'un quelconque des trois axes X hexagonaux de la couche initiale, avec un sens positif ou négatif du déplacement déterminé uniquement par la position du cation octahédrique dans la couche inférieure, et (c) le déplacement de la deuxième couche par $\pm b/3$ le long de Y_1 (normale à X_1) de la couche initiale, sans égard pour la position du cation octahédrique.

En supposant une géométrie hexagonale idéale, sans ordre des cations, et sans interéchange dans le même crystal des trois types possibles de superpositions des couches, on peut alors dériver douze polytypes standards (plus quatre enantimorphes) avec des périodicités variant entre une et six couches. Les déplacement relatifs le long des trois axes X conduisent aux mêmes séquences des couches dérivées pour les micas, soit 1M, $2M_1$, 3T, $2M_2$, $2Or$ et 6H. Les polytypes 1T et $2H_1$ résultent de la superposition directe des couches. Les déplacements des couches de $b/3$ conduisent aux polytypes connus sous la désignation 2T, 3R, $2H_2$ et 6R.

Les douze structures standards 1 : 1 peuvent être divisées en quatre groupes (A = 1M, $2M_1$, 3T; B = $2M_2$, $2Or$, 6H; C = 1T, 2T, 3R; D = $2H_1$, $2H_2$, 6R) pour les besoins d'identification. Les fortes réflections des rayon X servent à identifier chaque groupe et les réflections plus faibles différencient les trois structures au sein de chaque groupe. Des exemples des quatre groupes et de 9 des 12 structures individuelles ont été identifiées dans des spécimens naturels. La considération des quantités relatives d'attraction et de répulsion entre les ions dans les structures conduit à prédire la séquence de stabilité groupe C groupe D groupe A groupe B, qui s'accordent modérément aux abondances observées dans ces groupes structurels.

Kurzreferat—Die Polytypie in trioktaedrischen 1 : 1 Phyllosilikaten rührt von zwei veränderlichen Merkmalen im Gefüge her. (1) Die oktaedrischen Kationen können durchwegs in der gleichen Gruppierung von drei Stellungen angeordnet sein oder sie können in aufeinanderfolgenden Schichten jeweils zwischen zwei verschiedenen Gruppierungen der Stellungen abwechseln. (2) Die Wasserstoffbindung zwischen benachbarten Sauerstoff- und Hydroxyloberflächen aufeinanderfolgender Schichten kann durch drei verschiedene Stellungen der Schichten in Beziehung zu einander erhalten werden: (a) unmittelbare Überlagerung der Schichten, (b) Verschiebung der zweiten Schicht um $a/3$ entlang irgendeiner der drei hexagonalen X-Achsen der Ausgangsschicht, wobei eine positive oder negative Richtung der Verschiebung einzig durch die in der unteren Schicht eingenommene Gruppierung der oktaedrischen Kationen bestimmt wird, und (c) Verschiebung der zweiten Schicht um $\pm b/3$ entlang Y_1 (normal zu X_1) der Ausgangsschicht ungeachtet der eingenommenen oktaedrischen Kationgruppierungen.

Unter der Annahme idealer hexagonaler Geometrie, ohne Kationenregelung und ohne Vermischung innerhalb des gleichen Kristalls der drei möglichen Arten der Schichtüberlagerungen, lassen sich zwölf Normalpolytypen (plus vier Enantiomorphe) mit Periodizitäten zwischen einer und sechs Schichten ableiten. Relative Verschiebungen entlang der drei X-Achsen führen zu den bereits für die Glimmer abgeleiteten Schichtfolgen, nämlich 1M, $2M_1$, 3T, $2M_2$, $2Or$ und 6H. Die Polytypen 1T und $2H_1$ werden durch direkte Überlagerung von Schichten erhalten. Schichtverschiebungen um $b/3$ führen zu Polytypen mit der Bezeichnung 2T, 3R, $2H_2$ und 6R.

Die zwölf Normal 1 : 1 Gefüge können für Identifizierungszwecke in vier Gruppen eingeteilt werden (A = 1M, $2M_1$, 3T; B = $2M_2$, $2Or$, 6H; C = 1T, 2T, 3R; D = $2H_1$, $2H_2$, 6R). Die starken Röntgenreflexionen diesen zur Identifizierung der verschiedenen Gruppen, während die schwächeren Reflexionen zwischen den drei Strukturen innerhalb jeder Gruppe unterscheiden. Beispiele für alle vier Gruppen, sowie für 9 der zwölf Einzelgefüge konnten in natürlichen Proben aufgefunden werden. Eine Erwägung der relativen Beträge von Anziehung und Abstossung zwischen den Ionen in den jeweiligen Gefügen führt zu der vorhergesagten Stabilitätsfolge Gruppe C > Gruppe D > Gruppe A > Gruppe B, in ziemlich guter Übereinstimmung mit den beobachteten, mengenmässigen Vorkommen dieser Strukturgruppen.

Резюме—Политипия триоктаэдрических слоистых силикатов 1 : 1 обусловлена следующими двумя особенностями структуры. (1) Октаэдрические катионы могут занимать либо один и тот же из трех набор положений по всей структуре, либо, упорядоченно чередуясь, могут занимать два набора положений в последовательных структурных слоях. (2) Водородные связи между соседними кислородными и гидроксильными поверхностями последовательных слоев могут реализоваться при трех различных относительных положениях слоев: (а) прямое наложение слоев без смещения; (в) наложение слоев при смещении верхнего слоя на $a/3$ вдоль любой из трех гексагональных осей X нижнего слоя, причем положительное или отрицательное направление смещения однозначно определяется положением октаэдрических катионов нижнего слоя; (с) наложение слоев при смещении верхнего слоя на $\pm b/3$ вдоль оси $У_1$

(перпендикулярной X_1) нижнего слоя вне зависимости от положения октаэдрических катионов. При предположении гексагональной геометрии, отсутствия упорядочения катионов и невозможности сочетания в одном и том же кристалле 3-х упомянутых типов наложения слоев, могут быть выведены 12 независимых политипов (и 4 энантиоморфных) с периодичностью от одного до шести слоев на элементарную ячейку. Относительные смещения вгонь трех осей X приводят к образованию тех же последовательностей слоев, которые были выведены для слюд, а именно 1M, $2M_1$, 3T, $2M_2$, 20 и 6H. Политипы 1T и $2H_1$ получаются при прямом наложении слоев без смещения. Смещения слоев на $b/3$ приводят к образованию политипов, обозначаемых как 2T, 3R, $2H_2$ и 6R. В целях идентификации 12 полученных независимых структур могут быть разбиты на 4 группы (A=1M, $2M_1$, 3T; B=$2M_2$, 20, 6H; C=1T, 2T, 3R; D=$2H_1$, $2H_2$, 6R). Каждая группа имеет один и тот же набор сильных рентгеновских рефлексов, по которым может быть проведена идентификация различных групп; слабые рефлексы позволяют различать структуры внутри самих групп. При изучении природных образцов найдены представители всех четырех групп и 9-ти из 12-ти политипных структур. Анализ взаимного притяжения и отталкивания ионов в структурах позволил предсказать относительную устойчивость найденных групп, которая выражается следующей последовательностью: группа C> группа D> группа A> группа B, что находится в относительно хорошем соответствии с наблюдаемой распространенностью этих структурных групп в природе.